

Hydrological functioning of a field combining surface and subsurface drainage: from the water balance to the soil water pathways.

Arthur Gaillot¹, Célestine Delbart¹, Sébastien Salvador-Blanes¹, Pierre Vanhooydonck¹, Marc Desmet¹, Thomas Grangeon², Aurélie Noret³, and Olivier Cerdan²

¹Université de Tours

²Bureau de Recherches Géologiques et Minières

³Université Paris-Saclay

May 5, 2021

Abstract

Agricultural drainage networks increase hydrological connectivity from the field to the receiving environments. The response to the issue of surface water quality therefore implies an understanding of the hydrological processes related to drainage, particularly at the field scale. Drainage by tile drains and drainage ditch are the two most studied types at the plot scale. They can be complemented by temporary surface drains to improve the removal of surface runoff. The hydrological processes and functioning of tile-drained fields have been extensively studied at the event scale. However, few studies have been conducted over a full hydrological year and the description of water pathways in the soil generally relies on either exogenous tracer monitoring or irrigation experiments. In addition, only a few studies have been conducted on fields combining tile drainage and temporary surface drainage. In this study, high temporal resolution quantification of runoff from surface and subsurface drainage was conducted for a full year to establish one of the first water balances for a surface and subsurface drained field. Soil water pathways were studied under dry and saturated soil conditions tracing water by measuring stable isotope concentrations (¹⁸O and ²H) on rainwater, soil water, and surface and subsurface runoff. Runoff quantifications showed that surface drainage and subsurface drainage respectively evacuate 41% and 32% of the annual cumulated effective rainfall. The water balance highlights the importance of infiltrations to the deep horizons: 46% of the water transferred to the soil is not captured by the subsurface drains. Water tracing showed that rainwater was directly transferred to subsurface drains on dry soil, likely through macropores. On saturated soil, soil water present before the rain remains the main source of water to the subsurface drains, but event-rainwater also reaches the subsurface drains and can constitute up to 25% of the subsurface runoff volume.

Hydrological functioning of a field combining surface and subsurface drainage: from the water balance to the soil water pathways.

A. Gaillot^{1,2}, C. Delbart¹, S. Salvador-Blanes¹, P. Vanhooydonck¹, M. Desmet¹, T. Grangeon², A. Noret³, O. Cerdan².

¹ EA 6293 GéHCO - Université de Tours, Faculté des Sciences et Techniques, Tours, France

² Bureau de Recherches Géologiques et Minières, Département Risques et Prévention, 3 Avenue Claude Guillemin, Orléans, France

³ Université Paris-Saclay, CNRS, GEOPS, Orsay, 91405, France

Abstract

Agricultural drainage networks increase hydrological connectivity from the field to the receiving environments. The response to the issue of surface water quality therefore implies an understanding of the hydrolo-

gical processes related to drainage, particularly at the field scale. Drainage by tile drains and drainage ditch are the two most studied types at the plot scale. They can be complemented by temporary surface drains to improve the removal of surface runoff. The hydrological processes and functioning of tile-drained fields have been extensively studied at the event scale. However, few studies have been conducted over a full hydrological year and the description of water pathways in the soil generally relies on either exogenous tracer monitoring or irrigation experiments. In addition, only a few studies have been conducted on fields combining tile drainage and temporary surface drainage. In this study, high temporal resolution quantification of runoff from surface and subsurface drainage was conducted for a full year to establish one of the first water balances for a surface and subsurface drained field. Soil water pathways were studied under dry and saturated soil conditions tracing water by measuring stable isotope concentrations (^{18}O and ^2H) on rainwater, soil water, and surface and subsurface runoff. Runoff quantifications showed that surface drainage and subsurface drainage respectively evacuate 41% and 32% of the annual cumulated effective rainfall. The water balance highlights the importance of infiltrations to the deep horizons: 46% of the water transferred to the soil is not captured by the subsurface drains. Water tracing showed that rainwater was directly transferred to subsurface drains on dry soil, likely through macropores. On saturated soil, soil water present before the rain remains the main source of water to the subsurface drains, but event-rainwater also reaches the subsurface drains and can constitute up to 25% of the subsurface runoff volume.

Key words: tile drain, surface drainage, water balance, water tracing, soil water pathways, percolation.

1. INTRODUCTION

Subsurface drainage constitutes an artificial water pathway that directly links subsoil to surface waters. Since the 1950s, production-oriented agricultural policies have led to draining hydromorphic soils to increase the area of cultivated land and its yield (Musgrave, 1994). According to the last data of the International Commission on Irrigation and Drainage (2018), 11% of the arable lands of the world are drained. Two types of drainage are commonly used: drainage by digging ditches at the edge of the field and subsurface drainage by laying buried pipes.

At the watershed scale, one of the first drainage impact studied is the impact on flooding (Skaggs et al., 1994). In particular, drainage by tile drains reduces the intensity of floods that have a low return period, typically, less than 2 years (Nedelec, 2005). This is due to an increased transit time of water percolating through the soil to the tile drains in comparison to a direct transfer of water on the soil surface. Studies have also focused on the ecological and biological impact of drainage systems on receiving environments (Blann et al., 2009; Gilliam & Skaggs, 1986). Reducing subsurface drainage impact at the watershed scale implies to understand drainage impact at the field scale.

At the field scale, in temperate climates, the functioning of tile drains is generally highly seasonal (Arlot, 1999; Gramlich et al., 2018; Hirt et al., 2011; K.W. King et al., 2014). The decrease in evapotranspiration during the fall leads to the formation of a saturated zone in the soil. The saturated zone, or perched water table, is usually present from fall to spring. Zimmer, (1988) defines this period as a period of intense drainage during which runoff coefficients are at their maximum. During the rest of the year, the drains only flow during intense storm events. In addition, subsurface drainage has been shown to reduce surface runoff most of the time. For example, Arlot (1999), comparing drained and no-drained fields with Cambisol on altered shale, showed subsurface drainage represents 90% of the total runoff and decreases by a factor 10 to 20 the surface runoff. Grazhdani et al., (1996), in fields with clay loam, showed subsurface drainage increases the water yield by 34% but reduces surface runoff by 40%. In this case however, subsurface runoff contribution to the total runoff varied from 47% to 69%. The impact of drainage on surface runoff depends on the type of soil but also on the design of the drainage system. In lowland agricultural regions such as the Région Centre-Val-de-Loire in France, subsurface drainage is complemented by a third type of drainage: surface drainage by digging surface drainage rills (SDR). Contrary to tile drainage and ditches, SDRs are temporary: they are installed after seeding and destroyed by the first tillage following the harvest. This type of drainage is used to improve the evacuation of excess surface water and to direct surface runoff. It provides an additional water transfer pathway. Drainage by SDR is therefore likely to modify the hydrological functioning of the

field. However, to our knowledge, no work have been carried out on fields or watersheds with this type of drainage. Therefore, no water balance has been established for a surface and subsurface drained field.

Studies at the scale of the soil profile in drained contexts have shown that macropores are likely to be an important pathway for dissolved (King et al., 2015) and solid transfers (Michaud et al., 2019; Øygarden et al., 1997). Understanding the pathways of water flow in drained soils is essential to reduce the negative impacts of drainage. Water flow in soils can be categorized in two types of flow: one through the soil matrix (Skopp, 1981) and the other through macropores (Jarvis, 2007; McDonnell, 1990; Richard & Steenhuis, 1988). Matrix flow is generally slower than macropore flow, which is qualified as preferential flow. Macropores can have biological or structural origin and are distinguished from the rest of the porosity by the heterogeneity of their distribution (vertical and lateral), their large diameter and their strong connectivity. Geochemical tracing experiments and observation of water flow paths through the use of brilliant blue has highlighted the role of macropores in the hydrological functioning of drains (Stamm et al., 2002). This study showed that macropores enhance the connectivity between the surface and the drains. Using bromide tracing, Everts & Kanwar (1990) measured, during two irrigation experiments, that 29% and 20% of the total volume flowing out of the drain was from a preferential flow. Stone & Wilson (2006), using chloride tracing, measured a preferential flow contribution of 11% and 51% during two rainfall events. After two years of isotopic monitoring, Leaney et al. (1993) estimated that the share of preferential flow at the drain outlet was at least more than 80%. These studies underline the difficulty that persists in predicting the share of preferential flow reaching the drain during a rainfall event. A few studies have therefore looked for factors influencing the functioning of macropores. For example, Grant et al. (2019), by observing with brilliant blue the water pathways taken in two types of soils, have highlighted the influence of soil type on the flow of water through macropores: the preferential flow in a clayey soil is greater than in a sandy-silt soil. In addition to the soil properties, the functioning of macropores seems to be linked to the hydric state of the soil. Following blue-glow tracing experiments combined with high temporal resolution soil moisture measurements, Weiler & Naef (2003) showed that water circulation in macropores was dependent on the water content of the different horizons. The authors explained that the reason for this difference is due to exchanges between matrix and macropores. Moreover, they showed that the circulation of water in the macropores could either start at the level of a saturated horizon or from the soil surface when the rainfall intensity exceeded the infiltration capacity of the soil. Smith & Capel (2018), by monitoring the specific conductance of water at the drain outlet, have shown that even a light rainfall (< 5 mm) can lead to a preferential flow of rainwater through the macropores.

However, most of the studies concerning water flow in a drained context have focused on a few rainfall events without accounting for the seasonal variability of drain operation. In order to improve agricultural practices to reduce dissolved and solid exports from drains, it is preferable to determine the type of water flow in drained soils throughout the year, particularly with regard to variations in the hydric state of the soil.

Studies dealing with the different aspects of the hydrological functioning of subsurface drains reveal that:

- The hydrological functioning of field combining surface and subsurface drainage is rarely studied
- Most of the studies concerning subsurface drainage are conducted at the scale of the runoff event but few are conducted over longer periods or even over a full hydrological year.
- Uncertainties remain on the distribution between matrix and preferential flow according to the hydric stat of the soil.

In order to answer the questions raised by these gaps, the objectives of this study are:

- To establish the water hydric balance of a field with surface and subsurface drainage.
- To understand the influence of soil hydric conditions on the functioning of surface and subsurface drains under natural conditions over the course of a full hydrological year.
- To understand the influence of soil hydric conditions on water pathways in the soil.

To meet these objectives, we propose to quantify the surface and subsurface drainage flows of an agricultural field by measuring at high temporal resolution the flow rates at the outlet of drains over a whole hydro-

logical year. In parallel, we also propose to monitor the soil hydric state by tensiometric and piezometric measurements with high temporal resolution. Finally, the study of water pathways in the soil according to the hydric state of the soil will be addressed through isotopic tracing of water during a winter runoff event and a spring runoff event.

2. MATERIALS AND METHODS

2.1 Study site

The study site is a five hectares cultivated field characterised by a mean slope of 0.7%. The field is located in the 25 km² Louroux lowland catchment (0°45'20.43"E,47deg08'33.51"N) (Grangeon et al., 2017), in the Loire river basin around 250 km south-west of Paris, France (Figure1). The field is bordered by a ditch on the N-W and N-E sides, a farm road on the S-W side and adjacent to another crop field on the S-E side. During the study period, the field was cultivated with wheat; seeded on October 10th 2019 after a superficial tillage.

The field substratum is Helvetian shelly sands (Rasplus et al., 1982). A grain size analysis realized at the center of the field (Table 1) shows an abrupt change in clay content at about 40 cm depth: above 40 cm depth, soil has loamy clay texture and below 40 cm depth, soil is compact with a heavy clay texture. A soil augering campaign (52 points) confirmed the presence of a compact clay layer at 47.6 cm mean depth (30.0 to 85.0 cm). Redoximorphic features are observed from 25 cm depth, confirming the hydromorphic behaviour of the soil. This soil is classified as a Cambisol (FAO, 2014).

As in most fields of the catchment, two types of drainage are observed in the study site (i) a subsurface drainage with tile drains and (ii) a surface drainage with SDRs (Figure1).

For the subsurface drainage system, tile drains has been installed at 120 cm depth with a 10 m spacing during the 1980s. Two drain collectors of 16 cm diameter span the field (Figure 1). The main collector collects the runoff of 34 tile drains, i.e. 4.16 hectares and is connected to the ditch at the north of the field. The collector output is 16 cm above the bottom of the ditch and can be submerged during a runoff event. The second drain collector collects the runoff of 7 drains and drains other fields. The last cleaning of the drains occurred in 2017. Only the main drain collector is monitored, it drains 83% of the field.

After seeding operations, the farmer digs out a temporary artificial surface drainage rill network (SDR, figure 1). SDRs are U-shaped and shallow (15 cm). They either intersect the major slope or follow microthalwegs to enable the export of excess surface and hypodermic water to the surrounding ditch. These SDR network persist till the first tillage operation that follows the harvest. The SDR network is composed of primary SDR that are connected to a collector SDR, itself connected to the ditch network. The main collector SDR is connected to the N-E ditch and a second one is connected to the N-W ditch. The SDR collector drains 83% of the field.

2.2 Data acquisition

2.2.1 Hydrological and hydrodynamic measurements

Rainfall is monitored with an automatic rain gauge located at the northeast corner of the field (Figure 1). Rainfall is logged every five minutes with a 0.2 mm accuracy. A total of 722.0 mm was recorded during the study period from September 2019 to August 2020, which is representative of the average cumulated rainfall in the area (ca. 685 mm 1981-2010, MeteoFrance) (Figure 2). However, the spring and summer are drier (-19%) whereas the autumn and winter are more humid (+23%) than the average. Potential evapotranspiration (PET) was estimated at hourly time step from the Penman–Monteith equation accounting for the hourly average of air temperature, wind speed, solar radiation, humidity and atmospheric air pressure. All measurements for the PET estimation were logged at a weather station of the Louroux catchment located 2 km northeast of the study field.

At the output of the SDR collector, the runoff water level height is measured every minute with a 2 mm accuracy in a Venturi channel (Figure 3a) placed at the output of the furrow collector. The runoff discharge

is deduced from the water height using the constructor rating curve. An original device (Figure 3b) was designed to monitor the tile drain subsurface runoff flow. A horizontal PVC-siphon was placed in the continuity of the main drain collector output. At the extremity of the siphon, a doppler radar measured flow every minute. This set up allows the flow monitoring without flow modification and it allows measurements even when if the drain collector output is under water, a common situation in this region.

The soil hydric state was characterised by two types of measurements: the soil water tension on a plot on the study site and the upper depth of the saturated zone at 10 measuring points. The soil water tension was recorded every 10 minutes with autonomous WaterMark(r) tensiometers. Four groups of tensiometers were installed at a distance of 0.5, 1.5, 2.5 and 5 m of a subsurface tile drain axis. For each group, soil water tension was recorded at 15, 30 and 45 cm depth on each lines. Five manual tensiometers were installed to check the autonomous records. The upper limit depth of the saturated zone was recorded every 10 minutes from December 22th to June 7th with Mini-Diver probes compensated for atmospheric pressure using a Baro-Diver (Schlumberger Water Service) (Figure 1). The measurement accuracy is ± 1 cm H₂O. The Mini-Diver probes are installed in piezometers at a depth of 40 cm. The locations have been chosen with a stratified random sampling and probes are placed at the interdrain above the clayey horizon.

2.2.2 Runoff sampling and isotopic analysis

In order to study water pathways in the soil, two runoff events (Table 3) were selected, one during the period of intense drainage (event A, February 2nd) and the other occurring in late spring (event B, May 10th). These two events are representative of the runoff events of their respective period. These events was chosen because their representativeness and because the sampling realized. Stable isotope composition of soil water was only determined for the event A, i.e. when the soil water content was high enough to be sampled.

A rain collector is set next to the raingauge. During the runoff event sampling period, the rainfall is collected to represent only the study rainfall event by changing the rain collector just before and after the rainfall. Otherwise, the rainfall is collected by period of two weeks.

Surface and subsurface drainage runoff water is sampled using two automatic samplers. The sampling frequency depends on the runoff rate and it was manually adjusted for each event. For the subsurface runoff, the samples are taken at the beginning of the siphon (Figure 3) to avoid any discharge measurement perturbation. For the surface runoff, water is sampled at the middle of the “U” Venturi channel (Figure 3).

Soil water was sampled with ceramic cups. Four ceramic cups (15, 30, 45 and 80 cm depth) are parallel to and 3.5 m away from the tile drain axis. Two ceramic cups (30 cm depth) are perpendicular to and 1.5 m away from the drain axis. To sample soil water from the ceramic cups, a depression of 800 mbar was generated with a mannual vaccum pump.

Samples were filtered at the laboratory within a period of 24 hours after the sampling with 0.45 μ m cellulose acetate membranes. Stable isotopes of water were analysed by laser spectrometry with a Picarro L2120-i. The results are expressed using the conventional notation (δ as a deviation from the Vienna Standard Mean Ocean Water (V-SMOW)). The analytical error for ¹⁸O and ²H are ± 0.2 and δ^2 H rain signature during a rainfall event have not been determined. From October 2018 to October 2020, 39 rainwater samples were collected allowing to determine a Local Meteoric Water Line (LMWL) as follows:

$$\delta^2H = 7.46 \times \delta^{18}O + 5.61 \text{ (Equation 1)}$$

2.2.3 Water balance at the field scale

In the case of a small intensively instrumented experimental study area, such as the studied field, it may be possible to solve the complete water balance for hydrological research purpose (Ward and Robinson, 2000). The aim of the water balance in this study is to improve the knowledge of hydrological processes at the field scale.

A water balance was calculated using daily time step as follows:

$$S = P - RET - D - I \text{ (Equation 2)}$$

where ΔS is the variation of soil water storage in the horizon LA and S1, P is the rainfall, RET is the real evapotranspiration, D is the drainage factor, i.e. sum of surface and subsurface runoff and I is the infiltration from S1 to S2. All the terms are in millimeters. The RET was estimated from the PET and from the crop growth coefficient. The crop growth coefficient was estimated using degree-day and growth stages relation.

3. RESULTS

3.1 Runoff and rainfall seasonality

During the study period, the total runoff volume was 145.4 mm. Surface and subsurface drainage have contributions of the same magnitude with 82.0 mm runoff from surface drainage and 63.4 mm runoff from subsurface drainage. 88.0% of the surface runoff flow and 96.1% of the subsurface runoff flow occurred between November 2019 and March 2020. During this period, surface and subsurface drainage response to a rainfall event are different. The surface runoff flow only occurs intermittently, after a sequence of rainfall events whereas the subsurface runoff is continuous from early November to mid-January and the end of January to mid-March. This period is defined as an intense drainage period (Zimmer, 1988). In contrast, the period from April to August can be defined as a low drainage period.

The hydrological year is characterized by 108 rainfall events (Figure 4), and only 41 have led to a runoff. During the intense drainage period, 39 of the 53 rainfall events induced runoff. During, the low drainage period, 28 rainfall events occurred but only two generated runoffs. Moreover, two periods could be defined from the soil hydric state (Figure 5.): the whole soil is constantly saturated until mid-March and partially saturated only during storm events after this date.

The seasonality of the runoff events is consistent with the seasonality of the effective rainfall events (Figure 2) and thus with the variations of the soil hydric state (Figure 5). In the following, a focus on two rainfall events representative of the intense and low drainage periods will be performed. The aim is to provide the reader a detailed description of surface runoff and tile drain flows dynamics during these two periods

3.2 Intense drainage period (November 1st – March 20th)

During the intense drainage period, low intensity ([?] 2.4 mm h⁻¹) and low cumulative ([?] 1 mm) rainfall events can generate runoff, the drainage system is therefore particularly reactive.

3.2.1 Surface and subsurface runoff

From the rainfall, subsurface and surface runoff times series, several parameters characterizing the runoff as rainfall response are determined (Table 2). During the intense drainage period, the surface runoff always starts before the subsurface runoff. The times lag between the beginning of the rising limb of the surface runoff and the subsurface runoff ranges from 0.22 hours to 29.08 hours. The peak flow was superior to 2.01 L s⁻¹ for 50% of the surface runoff events, whereas the maximum peak flow recorded for the subsurface runoff is 1.7 L s⁻¹ (Table 2). During the intense drainage period, the surface runoffs are characterised by shorter reaction times (2.50 h), shorter durations (13.48 h) and higher flow (5.22 L s⁻¹) compared to subsurface runoffs (6.72, 27.43 and 0.81 L s⁻¹, respectively).

3.2.2 Soil saturation

According to the measurement of soil water tension, the soil was already saturated, at 15, 30 and 45 cm of depth in mid-November. It stayed saturated at all the depth until mid-March. A short period at the mid of January is characterised by a slight decrease of the water tension in the topsoil, due to ten days without rainfall. Moreover, between mid-November (date of installation of the Mini-diver® probes) and mid-March, the saturated zone is at 30 cm or higher below the soil surface during 75% of the time.

3.3.3 Water sources and pathways

The event of the February 2nd (event A, Table 3 and Figure 7) was selected to study water sources and pathway during a runoff event of the intense drainage period. During the 5 days prior the event A, 5 rainfall events occurred. A saturated zone is less than 6 cm below the soil surface before the event. The surface runoff occurs 22 min before subsurface runoff. Therefore, event A is characterized by the presence of a shallow saturated zone before the event, a surface runoff preceding the subsurface runoff and a high runoff coefficient.

The $\delta^{18}\text{O}$ and $\delta^2\text{H}$ composition of rainwater, soil water, surface and subsurface runoff are determined at low time-step during a storm event in order to identify water sources and pathways. No evaporation process can be identified from the isotopic signatures (Figure 6), thus, a variability of isotopic signature is due to a hydrological such as a change of water origin or mixing condition.

During the event A, the isotopic composition of rain, soil water, subsurface and surface runoff are significantly different (figure 6). The surface and subsurface runoff water isotopic composition are included between the composition of soil water and rain highlighting that surface and subsurface runoffs are a mixing between these two end-members. The ratio are different, the subsurface runoff is characterized by a higher proportion of soil water than the surface runoff, nevertheless, the proposition of soil water in the surface runoff is not negligible.

A two-end-member mixing analysis (EMMA) (Pinder & Jones, 1969) has been applied using isotopic signatures to estimate the proportion of soil water and rainwater contributing to the surface and subsurface runoffs. The isotopic composition of subsurface runoff before the flood event was considered as the end-member corresponding to pre-event soil water (-6.9 ± 0.2 to the soil water composition (figure 6)).

The isotopic composition of subsurface runoff varies along the storm event: during the rise of flow, the $\delta^{18}\text{O}$ of subsurface runoff tends toward the rain composition underlining a rainwater contribution. At the time of the peak flow, the proportion of rainwater in the subsurface flow is estimated at 30%. During the falling limb, the $\delta^{18}\text{O}$ decrease reveals an increase of soil water contribution : at the end of the sampling, the proportion of pre-event soil water in the subsurface runoff is estimated at 80%. For the surface runoff, the isotopic composition varies slightly except at the beginning of the storm event where the isotopic composition tend slightly toward the rainfall composition then stay constant. Thus, the surface and subsurface runoff are composed of 40% and 75% of pre-event soil water and 60% and 25% of rain water respectively.

2.3 Low drainage period (March 20th – August 31st)

During the low drainage period, only two rainfall events generated runoff (May 11th and June 4th). They are two storm events of 35.2 mm and 28.4 mm with maximum rainfall intensities of 14.4 mm h^{-1} and 60.0 mm h^{-1} , respectively. During the five days before these events, the cumulated rainfall was only 1.8 mm and 2.8 mm, respectively. Therefore, runoff events that occurred during the low drainage period are generated by rainfall events combining high cumulated rainfall, high rainfall intensities and very little antecedent rainfall in comparison with the intense drainage period.

2.3.1 Surface and subsurface runoff

For the two events occurred during the low drainage period, the reaction time of the subsurface tile drain are among the shortest of all the events of the year: 1h57 and 3h02 for the May 11th and the June 4th event, respectively (Table 4). The May 11th event is the only event of the year where the subsurface drain reacts before the surface drain: the surface runoff began 1h54 after the subsurface runoff.

2.3.2 Hydric state of the soil

The soil water tension started to decrease around mid-March, at the end of March, and at the beginning of April at 15, 30 and 45 cm depth, respectively. This period corresponds to a decrease of the effective rainfalls and is correlated with the end of the intense drainage period. Measurements of the depth of the saturated zone confirm these results: from mid-March, the saturated zone is present only when intense rainfall event

occurs and is always more than 14 cm below the soil surface. From April, cracks progressively appear at the soil surface, that is consistent with the decrease of the soil water tension.

2.3.3 Water sources and pathways

In order to study water pathways during the low drainage period, the runoff event that occurred on May 11th was selected (event B, Table 3 and Figure 7).

Before the event B, the soil water tension is -45 cbar at 45 cm depth. During event B, for the first time of the year, the surface runoff follows the subsurface runoff (1.9 h lag time). Moreover, compared to the event B, the runoff coefficient is particularly low : 9%.

During the event B, the subsurface runoff $\delta^{18}\text{O}$ was almost constant, ranging from -4.9 surface runoff $\delta^{18}\text{O}$ ranged from $-4.9(+0.2)$ runoff, surface runoff $\delta^{18}\text{O}$ variations indicate the rainwater $\delta^{18}\text{O}$ varied during the event. At the beginning of Event B, surface and subsurface runoffs $\delta^{18}\text{O}$ are similar. During the event, surface and subsurface runoffs $\delta^{18}\text{O}$ progressively become significantly different. It suggests that, at the TD was still drained rainwater of the beginning of the event.

4. DISCUSSION

4.1 Impact of subsurface drainage on the water balance

From Sept. 2019 to Aug. 2020, surface and subsurface flows represented 11.3% and 8.8% of the total annual rainfall, respectively. The simultaneous measurements of subsurface and surface drainage discharges during an entire year in a field drained by temporary artificial rill and tile drains is an originality of the present study. Previous studies quantifying both surface and subsurface drainage discharges have been conducted on fields only drained by tile drains (Schwab, G. O. et al., 1980; Skaggs et al., 1994; E. Turtola & Paaajanen, 1995; Eila Turtola et al., 2007). In these studies, surface runoff pathways are free. In the present study, surface runoff is oriented manmade SDRs. So the surface runoff measurement is realized for a precise area that is the same all along the study period. Nevertheless, present results suggest that the surface runoff guidance by artificial rills do not modify the relative contribution of the two drainage networks: some studies report that the subsurface runoff represents 34% to 68% of the total runoff.

In order to have a better understanding of the hydric functioning of the field, a water balance could be established for the year 2019-2020. The calculation of the water balance (Figure 8) was performed on a daily time step with the components presented in Equation 2: precipitation (P), real evapotranspiration (RET), surface and subsurface runoff (D), and soil infiltration. Soil infiltration is composed of two terms: the variation of the water stock of the LA and S1 surface horizons (ΔS) and the infiltration to the underlying horizon (I), from S1 to S2. As there is no measurement of the variation of the water stock of the LA and S1 horizons throughout the year, the variations were estimated. The hydric capacities of the horizons were estimated from a pedotransfer function proposed by Saxton (1986) and based on grain size. The horizons (LA+S1) have an estimated cumulative total available water of 75.68 mm. The estimation of water transfers to LA and S1 is based on the following assumptions:

- (H1) The water stock can not exceed the water stock at field capacity - (H2) The water stock can not be lower than the water stock at the permanent wilting point

In addition, the distribution of water inputs or losses is based on the following hypothetical processes:

- (H3) When the effective rainfall is positive, water input is first allocated to the LA and S1 horizons provided that it does not contradict assumption (H1), then to the S2 horizon.

- (H4) When the RET is higher than the rainfall, the water losses are allocated in priority to the LA and S1 horizons, provided that they do not contradict hypothesis (H2), and then to the S2 horizon.

- (H5) At the beginning of the hydrological year, the soil water content is considered to be close to or equal to the water content at the permanent wilting point, both for the (LA+S1) horizons and for the underlying horizon.

The discharges and stock changes calculated under these assumptions are presented in Figure 8. After the rains of September and October, the water content of the LA+S1 horizons reaches the water content of the field capacity. This is confirmed by manual tensiometer measurements taken in early November. Variations in the measured depth of the saturated zone even indicate that the LA and S1 horizons can be rapidly saturated during a rainfall event, which is consistent with a pre-event water content close to field capacity. Once the water content of the LA+S1 horizons reaches the field capacity water content, flows from both surface runoff and tile drains were monitored during some rainfall events. Flow from tile drains becomes continuous from late November to mid-December (Figure 5.). At the same time, water percolation from S1 to S2 begins.

This is consistent with manual measurements of soil tension: at 95 cm depth, soil water tension is divided by 4 between early November and mid-December. By mid-December, 62% of the volume of water infiltrated to S2 during the intense drainage period has percolated. Until this date, percolation from S1 to S2 can represent up to 96% of the daily precipitation. Little percolation was calculated in January, suggesting that the S2 horizon was saturated. At the end of the intense drainage period, the volume of water percolated from (LA+S1) to S2 is 1.4 times the volume of water drained: 193.8 mm and 139.5 mm, respectively. By mid-March, no tile drain flow was measured, because of decreased soil water content in the LA+S1 horizons. This result was confirmed by experimental measurements. From mid-March, the water stock in the LA and S1 horizons did not reach the water stock at field capacity and no transfer from S1 to S2 is calculated. S2 water stock progressively decreases from mid-March to the end of August. Over the entire hydrological year, S2 water stock increased by 50.7 mm and subsurface drainage captures 54% of the water transiting through the soil (Table 5).

The water balance highlights the importance of percolation from S1 to S2 in the distribution of flows within the field. In particular, it seems that the clayey S2 horizon plays a buffering role in the initiation of subsurface runoff: subsurface runoff intensifies when the storage capacity of the S2 horizon is reduced. However, almost the half of the flow is not intercepted by the subsurface drains.

All of the assumptions made for the calculation of the water balance appear to be consistent with the measurements made during the intense drainage period. However, these assumptions, and more particularly assumptions (H3) and (H4), are less suitable for the low drainage period. Indeed, the development of the crop and the intensity of evapotranspiration mean that water loss must certainly affect the LA/S1 and S2 horizons in a more distributed manner. In addition, the presence of cracks significantly modifies the distribution of water in the soil (Koivusalo et al., 1999) and may lead to direct flow to S2. The seasonal contrast of the soil water content in the superficial horizons suggest changes in soil structure that may have consequences on the soil water pathways. In the following part, soil water pathways under dry and wet conditions are described.

4.2 Soil water pathways and generation of runoffs

During the intense drainage period, a saturated zone is observed 75% of the time, 30 cm below the soil surface or higher. The quasi-permanent saturation of the soil leads to a low infiltration capacity and a continuous water pressure above tile drains. Before event A, most the entire soil profile was already saturated but the depth of the saturated zone decreased during the event to reach less than 1.6 cm. The closer to the soil surface the saturated zone is, the higher the subsurface runoff flow is: it suggests subsurface discharge variations are caused by variations of the water pressure above the drain. Moreover, as shown by water tracing, subsurface runoff results from the mixing of both rainwater and soil water. Such a transfer had also been observed by (Coulomb & Dever, 1994) at the beginning of the intense drainage season but not in the middle of the drainage season. The authors explain this difference by the saturation of macropores during the drainage season. Our results suggest that macroporosity was still active during the studied event of the intense drainage period. Thus, a preferential flow through the macropores is possible even when the soil is saturated. Concerning the surface runoff, surface drainage may be caused either by a refusal of infiltration or by a transfer of water from the first soil centimeters to the SDRs. Isotope water tracing shows that surface runoff is a mix of both soil water and rainwater. The presence of soil water in the surface runoff may be due to the increase of the saturated zone level and lateral subsurface flows. Following isotopuron transfer,

Haria *et al.* (1994) gave the same explanation and specified that a lateral flow circulated over an impeding layer. The presence of such a lateral flow is therefore also possible in our case. The lateral flow would then flow directly into the ditch at the edge of the field and could constitute a significant but unquantified part of the water balance.

During the low drainage period, soil moisture is constantly low. However, the studied event shows that a sufficiently intense event can generate surface and subsurface runoff. For such events, subsurface runoff occurs before surface runoff, proving that the process of rainwater transfer to subsurface drains is faster than the generation of surface runoff. Two reasons can be suggested: (i) the presence of the wheat cover that slows the surface runoff and (ii) a preferential vertical flow through macropores. Isotopic measurements support the hypothesis of preferential flow through the macroporosity but our results do not support any conclusion about the soil cover effect on the surface runoff. During the studied event, surface runoff is only composed of rainwater. The similarity of the isotopic signatures of surface and subsurface runoffs suggest the subsurface runoff is also only composed of rainwater. Moreover, cracks present at the soil surface before the event constitute a macroporosity that can support a direct water transfer from soil surface to tile drains. This result is consistent with the conclusions of the dry and isotopic tracers based studies conducted by (Øygarden *et al.*, 1997) and (Klaus *et al.*, 2013) in fields with similar soils. Moreover, these authors underlined the role of the macropores distribution and connectivity for the water transfer to tile drains.

4.3 Conceptualization of the monitored field dynamics

Rainfall-runoff events for intense drainage and low drainage periods can be described in four steps (Figure 9). During the intense drainage period: (1) Before the rainfall event: a saturated zone is present. The subsurface drain already flows. The drained water is the pre-event soil water, composed by previous rainwater. In-between the tile drains, the soil moisture above the saturated zone is between the field capacity and the saturation. (2) Surface runoff initiation and rise of the saturated zone level due to an increase of the water content in the topsoil. The rain water is rapidly transferred to the tile drains through the soil macroporosity. The rainfall event water increases the pressure on the pre-event soil water; thus the subsurface discharge increases. The subsurface runoff discharge increases progressively and contains both pre-event soil water and event rain water. (3) Drainage of the saturated zone: the upper limit of the saturated zone begins to drop. If close enough from the surface, the saturated zone can overflow and contribute to the surface drainage system. The subsurface runoff still contains pre-event soil water and event rain water but the proportion of pre-event soil water increases. (4) End of the event: the saturated zone is progressively drained by the subsurface system. Surface runoff stops within a few hours. Subsurface runoff decreases progressively to its pre-event discharge.

During the low drainage period: (1) Before the rainfall event: soil moisture is very low and cracks are visible at the soil surface. (2) Runoff initiation and formation of local saturated zones: the surface runoff is reduced by the crop cover. Only intense rainfall events can generate surface runoff. Moreover, cracks are the preferential pathways for rainwater from the soil surface to the subsurface drain. Therefore, subsurface drainage can begin before or at the same time as the surface runoff. A saturated zone is formed deep in the soil. (3) Drainage of the saturated zone: the saturated zone is quickly drained by the subsurface drains. Cracks collapse and are clogged by the soil particles eroded from the surface soil, or form the sides of the cracks. (4) End of the event: runoffs stop quickly after the end of the rainfall. The saturated zone is not present anymore after the end of the event. The size and width of some cracks have been reduced.

5. CONCLUSIONS

In this study, we established the water balance of a surface and subsurface drained field and compared the runoff processes of surface and subsurface drains according to the soil hydric status. The quantification of the surface and subsurface fluxes allowed to find the characteristics of the discharges of the drained fields. In our case, the period of intense drainage extends from November to March and corresponds to a period during which the saturated zone is close to the soil surface. During this period, most of the subsurface discharge is due to a slow matrix flow of water into the soil but macroporosity seems to be active and contributes

to up to 30% of the subsurface discharge. Thus, it appears that rapid flows of water in soil to subsurface drains are present throughout the year and regardless of the hydric state of the soil. When the entire soil profile is saturated, a slow matrix flow of water from the soil to the drains occurs and stays dominant as long as the soil moisture content is greater than the field capacity. Surface drainage seems mainly due to a saturation-excess runoff but when the saturated zone approaches the soil surface, water from the first few centimeters of the soil can be transferred to surface drains. Moreover, according to the water balance, 44% of the water transiting through the soil infiltrate into the S2 horizon. At the end of the intense drainage period, the decrease in water content of the LA and S1 horizons to below field capacity results in the discontinuation of base flow for subsurface drainage. From mid-march to August, subsurface tile drains, like surface drains, only operate during intense rainfall events. However, the subsurface discharge comes from a preferential flow through the macropores while surface drainage is only due to a refusal of infiltration.

The calculation of the water balance proposed in this study makes it possible to predict the hydrological functioning of the drained field for the period of intense drainage. More particularly, it constitutes a model that makes it possible to anticipate the initiation of subsurface drainage. Provided that the variability of the soils and the characteristics of the drainage networks of the other fields in the watershed are taken into account, the simplicity of setting up this model should make it possible to extrapolate it to other fields. The application of this model on all the drained fields could then lead to the understanding of the hydrological functioning of the watershed and participate in the study of dissolved and particulate transfers from the fields to the watershed.

Moreover, according to the soil hydric state, water sources variations of subsurface runoff can be one of the factors explaining the variation in dissolved and solid transfers over the year in drained systems. Concerning surface drainage by digging SDRs, it can be observed that, in addition to the runoff process usually encountered in drained fields, there is a lateral flow of water from the soil to the SDRs when the saturated zone reaches the depth of the SDR. Such a flow is therefore likely to be associated with transfers of dissolved substances stored in the first few centimeters of soil.

ACKNOWLEDGMENTS

The authors acknowledge the technical support of PANOPLY (Plateforme ANalytique géOsciences Paris-saclay), Paris-Saclay University, France.

REFERENCES

- Arlot, M.-P. (1999). *Nitrate dans les eaux. Drainage acteur, drainage témoin ?* These de doctorat de l'Université Paris 6.
- Blann, K. L., Anderson, J. L., Sands, G. R., & Vondracek, B. (2009). Effects of Agricultural Drainage on Aquatic Ecosystems : A Review. *Critical Reviews in Environmental Science and Technology* ,39 (11), 909-1001. <https://doi.org/10.1080/10643380801977966>
- C. J. Everts & R. S. Kanwar. (1990). Estimating preferential flow to a subsurface drain with tracers. *Transactions of the ASAE* ,33 (2), 0451-0457. <https://doi.org/10.13031/2013.31350>
- Coulomb, C., & Dever, L. (1994). Evolution saisonniere des modalites de transfert d'eau et de solutes dans un sol argileux draine : Etude isotopique et chimique. *Hydrological Sciences Journal* ,39 (3), 217-233. <https://doi.org/10.1080/02626669409492739>
- Gilliam, J. W., & Skaggs, R. W. (1986). Controlled Agricultural Drainage to Maintain Water Quality. *Journal of Irrigation and Drainage Engineering* , 112 (3), 254-263. [https://doi.org/10.1061/\(ASCE\)0733-9437\(1986\)112:3\(254\)](https://doi.org/10.1061/(ASCE)0733-9437(1986)112:3(254))
- Gramlich, A., Stoll, S., Stamm, C., Walter, T., & Prasuhn, V. (2018). Effects of artificial land drainage on hydrology, nutrient and pesticide fluxes from agricultural fields – A review. *Agriculture, Ecosystems & Environment* , 266 , 84-99. <https://doi.org/10.1016/j.agee.2018.04.005>

- Grangeon, T., Maniere, L., Foucher, A., Vandromme, R., Cerdan, O., Evrard, O., Pene-Galland, I., & Salvador-Blanes, S. (2017). Hydro-sedimentary Dynamics of a Drained Agricultural Headwater Catchment : A Nested Monitoring Approach. *Vadose Zone Journal* ,16 (12), 0. <https://doi.org/10.2136/vzj2017.05.0113>
- Grant, K. N., Macrae, M. L., & Ali, G. A. (2019). Differences in preferential flow with antecedent moisture conditions and soil texture : Implications for subsurface P transport. *Hydrological Processes* , 33 (15), 2068-2079. <https://doi.org/10.1002/hyp.13454>
- Grazhdani, S., Jacquin, F., & Sulce, S. (1996). Effect of subsurface drainage on nutrient pollution of surface waters in south eastern Albania. *Science of The Total Environment* , 191 (1-2), 15-21. [https://doi.org/10.1016/0048-9697\(96\)05168-6](https://doi.org/10.1016/0048-9697(96)05168-6)
- Haria, A. H., Johnson, A. C., & Bell, J. P. (1994). Water movement and isotoproturon behaviour in a drained heavy clay soil : 1. Preferential flow processes. *Journal of Hydrology* , 14.
- Hirt, U., Wetzig, A., Devandra Amatya, M., & Matranga, M. (2011). Impact of Seasonality on Artificial Drainage Discharge under Temperate Climate Conditions. *International Review of Hydrobiology* ,96 (5), 561-577. <https://doi.org/10.1002/iroh.201111274>
- Jarvis, N. J. (2007). A review of non-equilibrium water flow and solute transport in soil macropores : Principles, controlling factors and consequences for water quality. *European Journal of Soil Science* ,58 (3), 523-546. <https://doi.org/10.1111/j.1365-2389.2007.00915.x>
- King, Kevin W., Williams, M. R., Macrae, M. L., Fausey, N. R., Frankenberger, J., Smith, D. R., Kleinman, P. J. A., & Brown, L. C. (2015). Phosphorus Transport in Agricultural Subsurface Drainage : A Review. *Journal of Environment Quality* , 44 (2), 467. <https://doi.org/10.2134/jeq2014.04.0163>
- King, K.W., Fausey, N. R., & Williams, M. R. (2014). Effect of subsurface drainage on streamflow in an agricultural headwater watershed. *Journal of Hydrology* , 519 , 438-445. <https://doi.org/10.1016/j.jhydrol.2014.07.035>
- Klaus, J., Zehe, E., Elsner, M., Kulls, C., & McDonnell, J. J. (2013). Macropore flow of old water revisited : Experimental insights from a tile-drained hillslope. *Hydrology and Earth System Sciences* ,17 (1), 103-118. <https://doi.org/10.5194/hess-17-103-2013>
- Leaney, F. W., Smettem, K. R. J., & Chittleborough, D. J. (1993). Estimating the contribution of preferential flow to subsurface runoff from a hillslope using deuterium and chloride. *Journal of Hydrology* , 147 (1-4), 83-103. [https://doi.org/10.1016/0022-1694\(93\)90076-L](https://doi.org/10.1016/0022-1694(93)90076-L)
- McDonnell, J. J. (1990). A Rationale for Old Water Discharge Through Macropores in a Steep, Humid Catchment. *Water Resources Research* ,26 (11), 2821-2832. <https://doi.org/10.1029/WR026i011p02821>
- Michaud, A. R., Poirier, S.-C., & Whalen, J. K. (2019). Tile Drainage as a Hydrologic Pathway for Phosphorus Export from an Agricultural Subwatershed. *Journal of Environmental Quality* , 48 (1), 64-72. <https://doi.org/10.2134/jeq2018.03.0104>
- Musgrave, M. E. (1994). Waterlogging Effects on Yield and Photosynthesis in Eight Winter Wheat Cultivars. *Crop Science* , 34 (5), 1314-1318. <https://doi.org/10.2135/cropsci1994.0011183X003400050032x>
- Nedelec, Y. (2005). *Interactions en crue entre drainage souterrain et assainissement agricole* . ENGREF (AgroParisTech). tel-00009180.
- Oygarden, L., Kvaerner, J., & Jenssen, P. D. (1997). Soil erosion via preferential flow to drainage systems in clay soils. *Geoderma* ,76 (1-2), 65-86. [https://doi.org/10.1016/S0016-7061\(96\)00099-7](https://doi.org/10.1016/S0016-7061(96)00099-7)
- Pinder, G. F., & Jones, J. F. (1969). Determination of the ground-water component of peak discharge from the chemistry of total runoff. *Water Resources Research* , 5 (2), 438-445. <https://doi.org/10.1029/WR005i002p00438>

- Rasplus, L., Macaire, J. J., & Alcaide, G. (1982). *Carte geologique de Blere au 1:5000, Editions BRGM* .
- Richard, T. L., & Steenhuis, T. S. (1988). Tile drain sampling of preferential flow on a field scale. *Journal of Contaminant Hydrology* , 3 (2-4), 307-325. [https://doi.org/10.1016/0169-7722\(88\)90038-1](https://doi.org/10.1016/0169-7722(88)90038-1)
- Schwab, G. O., Fausey, N. R., & Kopcak, D. E. (1980). Sediment and Chemical Content of Agricultural Drainage Water. *Transactions of the ASAE* , 23 (6), 1446-1449. <https://doi.org/10.13031/2013.34796>
- Skaggs, R. W., Breve, M. A., & Gilliam, J. W. (1994). Hydrologic and water quality impacts of agricultural drainage*. *Critical Reviews in Environmental Science and Technology* , 24 (1), 1-32. <https://doi.org/10.1080/10643389409388459>
- Skopp, J. (1981). Comment on Micro-, Meso- and Macroporosity of Soil. *Soil Science Society of America Journal* , 45 , 1246.
- Smith, E. A., & Capel, P. D. (2018). Specific Conductance as a Tracer of Preferential Flow in a Subsurface-Drained Field. *Vadose Zone Journal* , 17 (1), 170206. <https://doi.org/10.2136/vzj2017.11.0206>
- Stamm, C., Sermet, R., Leuenberger, J., Wunderli, H., Wydler, H., Fluhler, H., & Gehre, M. (2002). Multiple tracing of fast solute transport in a drained grassland soil. *Geoderma* , 109 (3-4), 245-268. [https://doi.org/10.1016/S0016-7061\(02\)00178-7](https://doi.org/10.1016/S0016-7061(02)00178-7)
- Stone, W. W., & Wilson, J. T. (2006). Preferential Flow Estimates to an Agricultural Tile Drain with Implications for Glyphosate Transport. *Journal of Environmental Quality* , 35 (5), 1825-1835. <https://doi.org/10.2134/jeq2006.0068>
- Turtola, E., & Paajanen, A. (1995). Influence of improved subsurface drainage on phosphorus losses and nitrogen leaching from a heavy clay soil. *Agricultural Water Management* , 28 (4), 295-310. [https://doi.org/10.1016/0378-3774\(95\)01180-3](https://doi.org/10.1016/0378-3774(95)01180-3)
- Turtola, Eila, Alakukku, L., Uusitalo, R., & Kaseva, A. (2007). Surface runoff, subsurface drainflow and soil erosion as affected by tillage in a clayey finish soil. *Agricultural and Food Science* , 16 , 332-351.
- Weiler, M., & Naef, F. (2003). An experimental tracer study of the role of macropores in infiltration in grassland soils. *Hydrological Processes* , 17 (2), 477-493. <https://doi.org/10.1002/hyp.1136>
- Zimmer, D. (1988). *Transferts hydriques en sols drainees par tuyaux enterres. Comprehension des debites de pointe et essai de typologie des schemas d'ecoulement*. These Universite Paris VI, Science du sol. CEMAGREF. 325 p.

Horizon	Depth	Clay (%)	Silt (%)	Sand (%)
LA	0-20 cm	26.5	41.5	32.0
S1	20-40 cm	35.5	40	24.5
S2	>40 cm	55.0	32	13.0

Table 1. Particle size of each soil horizon of the studied field.

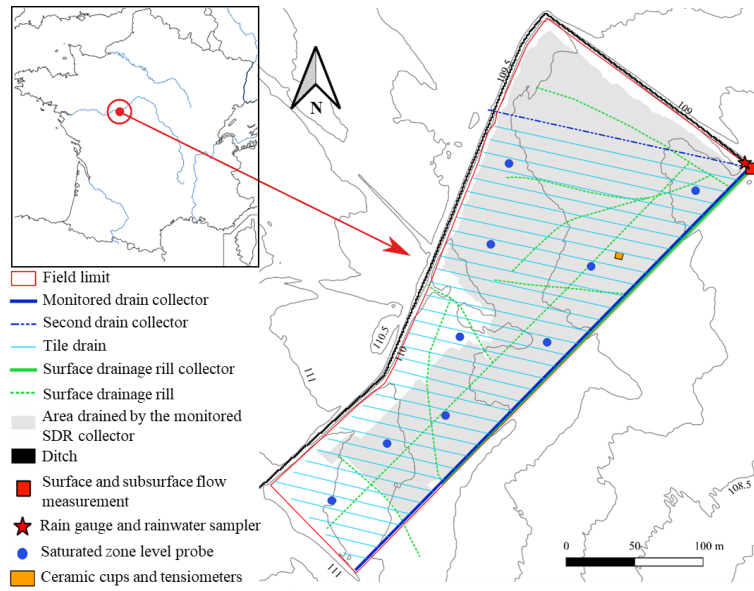


Figure 1. Description of the study field. The surface drainage rill collector is superimposed to the tile drain collector.

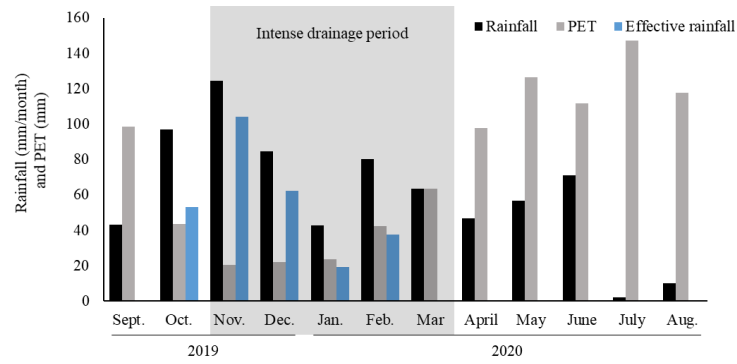


Figure 2. Monthly rainfall and PET from September 2019 to August 2020. Rainfall was measured at the study field and PET was estimated from a weather station located 2 km northeast of the study field.

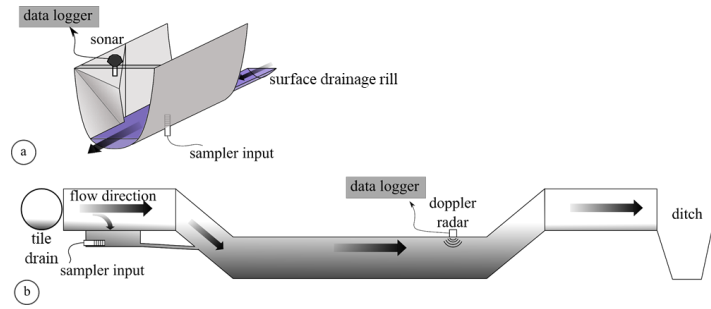


Figure 3. Schema of the instrumentation for flow measurements and water sampling of surface runoff (a) and the subsurface runoff (b).

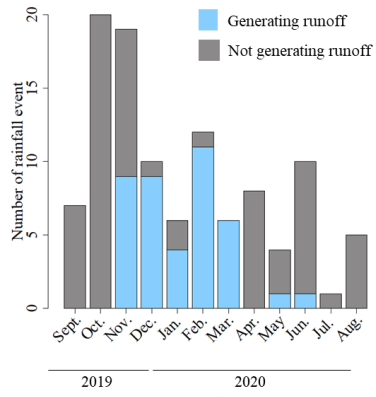


Figure 4. Number of rainfall events per month

	Subsurface runoff			Surface runoff		
	Minimum	Mean	Maximum	Minimum	Mean	Maximum
Peak flow (L s ⁻¹)	0.16	0.81	1.82	0.08	5.22	23.94
Volume (m ³)	4.63	43.25	135.47	1.28	79.79	626.04
Reaction time [†] (h)	1.23	6.72	30.77	0.42	2.50	11.75
Event duration (h)	9.00	27.43	88.00	2.50	13.48	28.00

Table 2. Hydrological characteristics of the subsurface (A) and surface (B) runoffs recorded during the intense drainage period. †Reaction time described here is the time difference between the rainfall barycenter and the start of the flow increase.

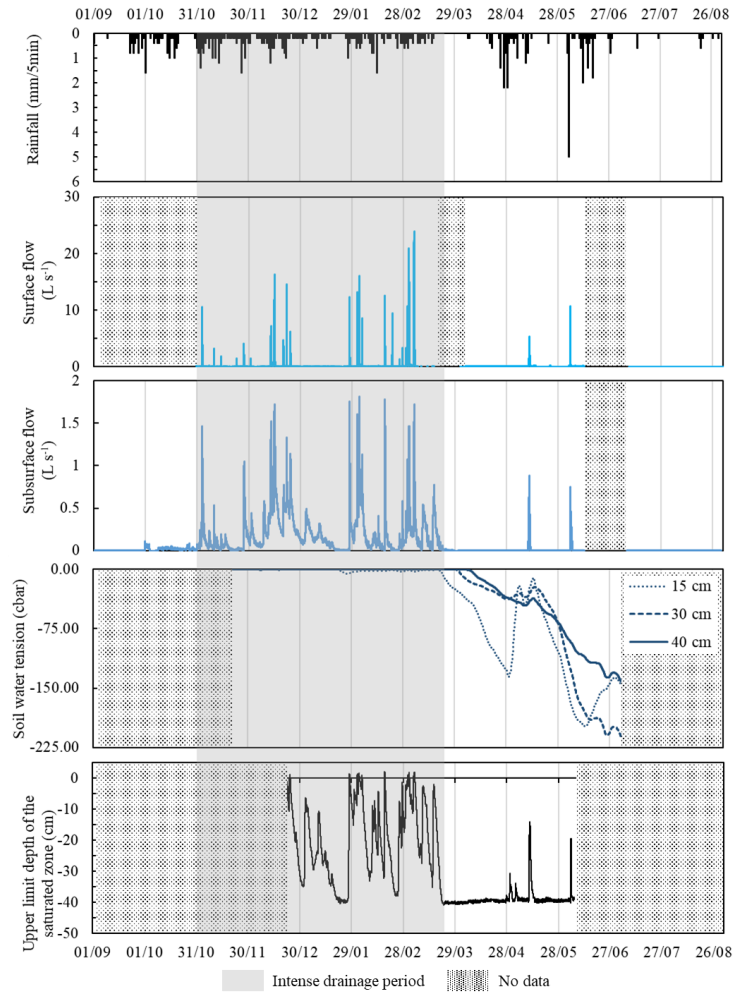


Figure 5. Rainfall, surface and subsurface runoff flows, soil water tension and average depth of the upper limit of the saturated zone measured during the study year. Soil water tension was measured at 15, 30 and 45 cm depth between two subsurface tile drains.

Event		Event A 02/02/2020	Event B 11/05/2020
Cumulative rainfall (mm)		9.4	35.2
Rainfall duration (h)		9.67	13.25
Maximum rainfall intensity (mm/5 min)		4.8	14.4
Pre-event rainfall (mm/48 h)		8.0	1.6
Pre-event rainfall (mm/5 days)		13.8	1.8
Total runoff (m ³)		293.8	132.3
Runoff coefficient (%)		75.3	9.6
Subsurface runoff	Peak flow (L s ⁻¹)	1.82	0.89
	Volume (m ³)	97.85	30.36
	Reaction time [†] (h)	2.28	1.95
	Rising limb (h)	5.38	1.85
	Recessional limb (h)	23.62	16.15
	Runoff duration (h)	29.00	18.00
Surface runoff	Peak flow (L s ⁻¹)	16.08	5.36
	Volume (m ³)	196.02	102.01
	Reaction time [†] (h)	1.92	3.85
	Rising limb (h)	5.42	3.42
	Recessional limb (h)	18.58	13.58
	Runoff duration (h)	24.00	17.00

Table 3. Hydrological characteristics of the two studied events. The event A is an event occurred during the intense drainage period and the event B occurred during the low drainage period. [†]Reaction time described here is the time difference between the rainfall barycenter and the start of the flow increase.

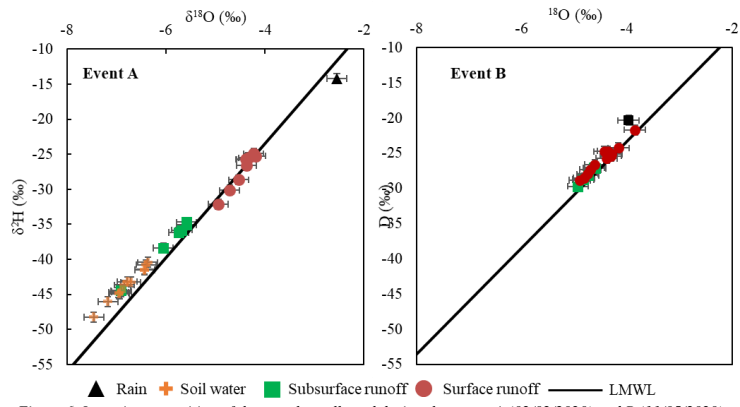


Figure 6. Isotopic composition of the samples collected during the events A (02/02/2020) and B (11/05/2020).

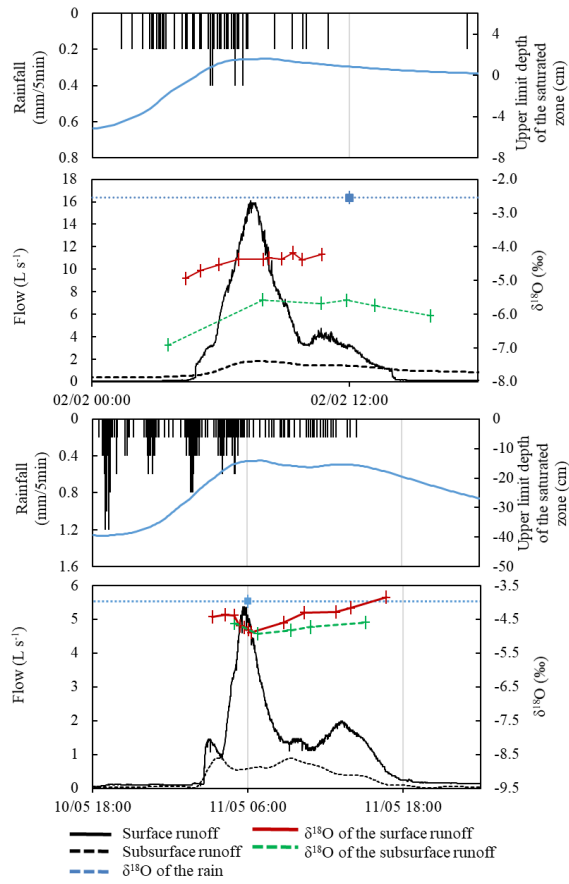


Figure 7. Rainfall, surface and subsurface runoff flows and $\delta^{18}\text{O}$ of rainfall, surface and subsurface runoffs for events A and B.

	Subsurface runoff		Surface runoff	
	Minimum	Maximum	Minimum	Maximum
Peak flow (L s⁻¹)	0,82	0,89	8,05	10,74
Volume (m³)	23,88	30,36	83,91	102,01
Reaction time[†] (h)	1.95	3.13	0.67	3.85
Rising limb (h)	1.85	2.13	0.67	3.42
Recessional limb (h)	16.15	23.37	4.33	13.58
Event duration (h)	18.00	25.50	5.00	17.00

Table 4. Hydrological characteristics of the subsurface (A) and surface (B) runoffs recorded during the low drainage period. †Reaction time described here is the time difference between the rainfall barycenter and the start of the flow increase.

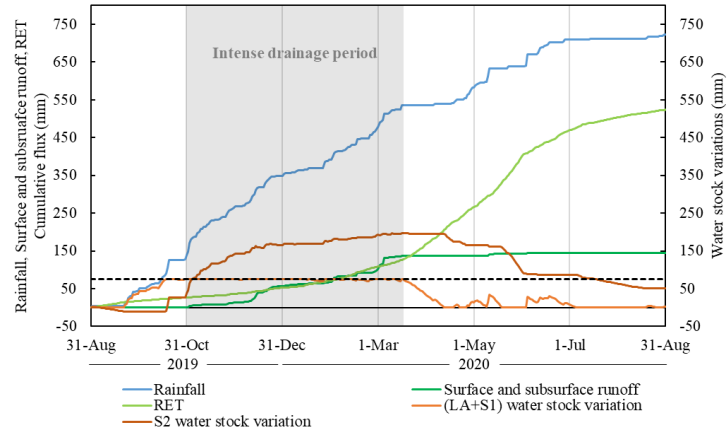


Figure 8. Variations of the water balance terms during the study period. "Effective rainfalls" represents the difference between the rainfalls and the ETR, "Surface and subsurface runoffs" represents the total runoff measured. "(LA+S1) water stock variation" represents the estimated water stock variation of the horizons LA and S1, "Variations of S2 water stock" represents the transfer from S1 to S2 or from S2 to S1. Variations of water stocks are the difference between the stock on September 1st and the stock on the given date. The black dot line represent the field capacity water stock of (LA+S1).

Water balance component		Cumulative volume (mm)
Rainfall		722.0
RET		523.6
Runoff	Surface drainage	82.0
	Subsurface drainage	63.4
LA and S1 water stock variation		2.3
Infiltration to S2		50.7

Table 5. Cumulative water balance components measured and estimated between September 1st 2019 and August 31st 2020

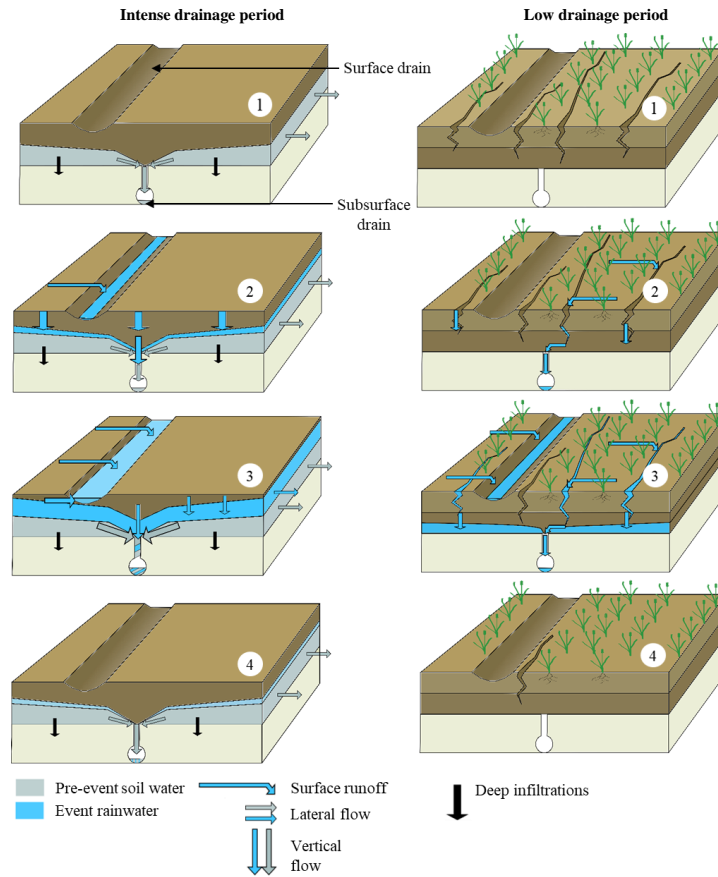


Figure 9. Conceptual model of the soil water pathways during the intense drainage and low drainage periods.